Acta Crystallographica Section C
Crystal Structure Communications
ISSN 0108-2701

EuI_2, a low-temperature europium(II) iodide phase

Michael Krings, Michael Wessel and Richard Dronskowski*

Institute of Inorganic Chemistry, RWTH Aachen University, Landoltweg 1, D-52056 Aachen, Germany
Correspondence e-mail: drons@hal9000.ac.rwth-aachen.de

Received 26 August 2009
Accepted 23 September 2009
Online 30 September 2009

Light-yellow europium(II) diiodide, prepared by the low-temperature reaction of europium and ammonium iodide in liquid ammonia at 200 K and characterized by high-resolution X-ray powder diffraction, represents a new phase for EuI_2 that adopts an orthorhombic *Pnma* structure with all three atoms lying on 4*c* positions (.*m*.). It is isotypic with SrI_2(IV). Temperature-dependent X-ray measurements performed to investigate the thermal stability of the new phase show that it decomposes irreversibly to amorphous material around 673 K. Total-energy density-functional calculations using the generalized gradient approximation suggest this to be the ground-state structure of EuI_2.

Comment

Because of the exceptional luminescence properties of Eu^{2+} ions, there is ongoing interest in synthetic techniques to generate europium(II) compounds easily at high purities. During a low-temperature synthesis of europium(II) iodide we found a new phase of this compound.

Currently, there are three well-described phases of europium(II) iodide: EuI_2 crystallizing in $P2_1/c$ (Bärnighausen & Schulz, 1969) and in *Pbca* (Bärnighausen & Schulz, 1969), and EuI_2 synthesized at high pressure crystallizing in *Pnma* (Beck, 1979). In 1989 (Liu & Eick, 1989), a new strontium(II) iodide structure in *Pnma*, called SrI_2(IV), was suggested. It was also mentioned by these authors that this structure was known for SmI_2 and EuI_2, but the details were never published. In 1995 (Wang *et al.*, 1995), this same europium(II) iodide was reported, too, but the phase was not stable at ambient temperature and could only be stabilized through 'high-pressure treatment', despite the fact that its molar volume is larger than those of all other phases. We now report a simple low-temperature route to this EuI_2 phase, which should indeed be called EuI_2(IV) by analogy with SrI_2(IV).

The compound crystallizes in the centrosymmetric orthorhombic space group *Pnma* with all three symmetry-inequivalent atoms situated on 4*c* positions (.*m*.) (Fig. 1). The structure is built up by edge-sharing polyhedra. The sevenfold coordination of Eu^{2+}, resulting in monocapped trigonal prisms, is typical for the europium(II) iodides. In the coordination polyhedron, a mirror plane passes through atoms $I1^{i}$, $I1^{ii}$, $I2^{iii}$ and Eu1, such that there are four different Eu—I bond lengths with an average of 3.35 Å (Fig. 2; symmetry codes given in Fig. 2).

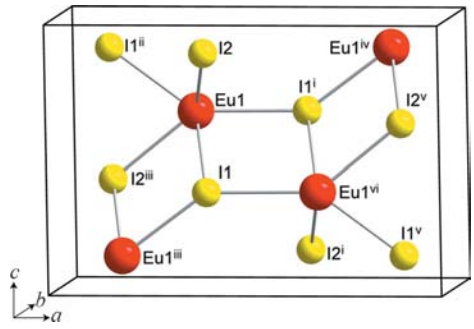

Figure 1
The unit cell of the title compound, with all atoms drawn as spheres of arbitrary radii. [Symmetry codes: (i) $-x+1, y+\frac{1}{2}, -z+1$; (ii) $-x+\frac{1}{2}, -y+1, z+\frac{1}{2}$; (iii) $-x+\frac{1}{2}, -y+1, z-\frac{1}{2}$; (iv) $x+\frac{1}{2}, -y+\frac{3}{2}, -z+\frac{3}{2}$; (v) $x+\frac{1}{2}, -y+\frac{1}{2}, -z+\frac{3}{2}$; (vi) $-x+1, y-\frac{1}{2}, -z+1$.]

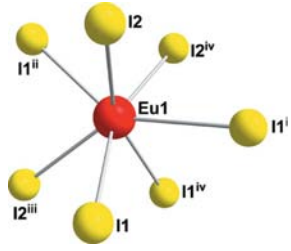

Figure 2
Schematic view of the EuI_7 polyhedron. Atoms Eu1, $I1^{i}$, $I1^{ii}$ and $I2^{iii}$ form a mirror plane passing through the polyhedron. [Symmetry codes: (i) $-x+1, y+\frac{1}{2}, -z+1$; (ii) $-x+\frac{1}{2}, -y+1, z+\frac{1}{2}$; (iii) $-x+\frac{1}{2}, -y+1, z-\frac{1}{2}$; (iv) $x, y+1, z$.]

To compare the four different structures, the packing of the EuI_7 polyhedra must be considered. In the EuI_2(IV) phase, the structure is built up by edge-sharing polyhedra forming parallel two-dimensional layers within the *bc* plane. The layers are connected through additional edge-sharing of the monocapped site. EuI_2 in $P2_1/c$ and *Pbca* exhibit very similar packings, in which the polyhedra are tilted such that the layer structure is broken up into a three-dimensional network of edge- and corner-sharing polyhedra. The high-pressure EuI_2 structure in *Pnma* contains strongly distorted EuI_7 polyhedra forming a dense three-dimensional network. There is no obvious relationship between the two structures crystallizing in *Pnma*.

For thermochemical analysis, temperature-dependent X-ray diffraction was performed using a Huber Guinier G644 diffractometer in the temperature range 300–773 K (Fig. 3). It is obvious that the phase starts decomposing at about 640 K, where all four reflections diminish in intensity. After heating, the resulting compound was cooled slowly to room tempera-

  doi:10.1107/S0108270109038542

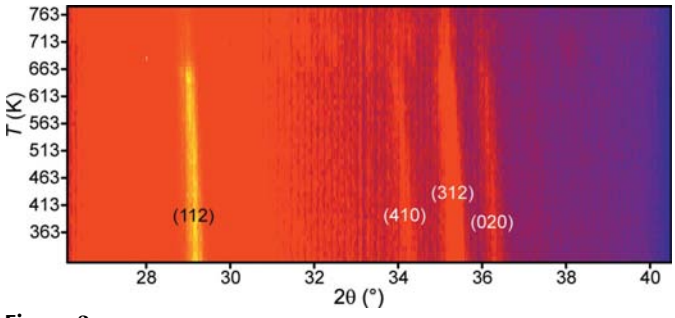

Figure 3
The temperature-dependent X-ray powder diffraction of EuI_2(IV). In the electronic version of the paper, high and low absolute intensities are displayed in yellow and blue, respectively.

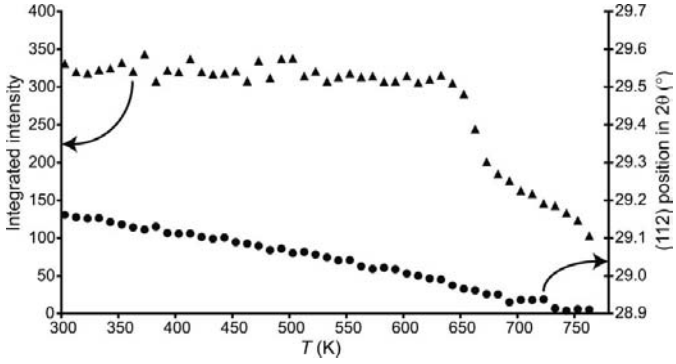

Figure 4
Plot of the integrated intensity (triangles) and the position of the (112) reflection (circles) *versus* temperature. At temperatures above 680 K, the linear decrease of the position of the (112) reflection and the trend of the integrated intensity are interrupted.

ture but the reflections of the original phase did not reappear; instead, the unstructured diffraction data point towards amorphous EuI_2. Thus, the phase transition is irreversible because EuI_2(IV) seemingly does not recrystallize from a high temperature.

Fig. 4 displays the course of the integrated intensity of the (112) reflection *versus* temperature, which matches the steady increase in the lattice parameters due to higher thermal motion. To determine the decomposition temperature more reliably, an exponential fit according to $I_{\rm Bragg} = a(T_c - T)^b$ was performed using the integrated intensities of the (112) reflections at different temperatures; the critical temperature T_c equals the decomposition temperature. On the basis of the data points up to 680 K, the parameters arrive at a = 250 (15) K^{-1}, a decomposition temperature of T_c = 673 (1) K and b = 0.034 (7). Data at higher temperatures were not taken into account because of complicated behaviour that may be due to inhomogeneous heating of the sample.

All four europium iodides in which Eu^{2+} experiences sevenfold coordination were theoretically compared by means of total-energy density-functional calculations. The results (Fig. 5) corroborate the experimental results. EuI_2 in *Pnma* obtained at high pressure and high temperature lies 11–16 kJ mol^{-1} higher in energy than the other phases and has the lowest volume. EuI_2 in *Pbca* and $P2_1/c$ may be obtained using similar experimental conditions, and the theoretical calculations show that they are close to each other in energy and volume. The low-temperature EuI_2(IV) phase, also crystallizing in *Pnma*, has the highest volume but lies lowest in energy.

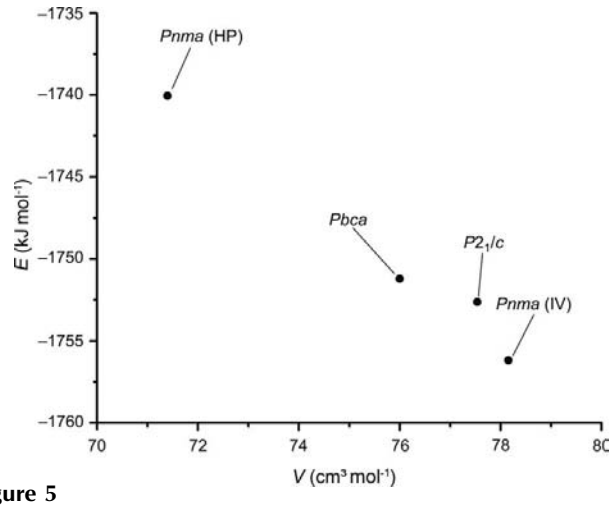

Figure 5
Energy–volume plot of the four known EuI_2 phases on the basis of density-functional (GGA) calculations.

Experimental

All manipulations were performed under a clean argon atmosphere. Europium(II) iodide was prepared according to the literature procedure of Howell & Pytlewski (1969) by dissolving two equivalents of oven-dried ammonium iodide in liquid ammonia in a Schlenk flask cooled by an ethanol–dry-ice mixture. The ammonia was condensed through a cooling finger placed on the Schlenk flask. One equivalent of elemental europium was added and the reaction started immediately. After the reaction was complete and no more hydrogen gas was produced, the solvent was allowed to evaporate by removing the cooling bath. The light-yellow product was heated to 473 K for 12 h to remove any residual ammonia and to improve crystallization.

Crystal data

EuI_2
M_r = 405.76
Orthorhombic, *Pnma*
a = 12.2665 (11) Å
b = 4.8875 (4) Å
c = 8.3697 (8) Å
V = 501.78 (8) $Å^3$
Z = 4
Cu $K\alpha_1$ radiation
μ = 184.46 mm^{-1}
T = 293 K
Specimen shape: cylinder
0.3 × 0.3 × 0.3 mm
Specimen prepared at 101.3 kPa
Specimen prepared at 200 K
Particle morphology: powder, light yellow

Data collection

Stoe Stadi MP diffractometer
Specimen mounting: capillary tube
Specimen mounted in transmission mode
Scan method: step
$2\theta_{\rm min}$ = 5.0, $2\theta_{\rm max}$ = 109.0°
Increment in 2θ = 0.02°

Refinement

R_p = 1.482
R_{wp} = 1.912
R_{exp} = 1.288
R_B = 8.093
S = 1.49
Wavelength of incident radiation: 1.540590 Å
Excluded region(s): none
Profile function: pseudo-voigt
379 Bragg reflections
20 parameters
Preferred orientation correction: none

Table 1
Selected bond lengths (Å).

Eu1—I1	3.379 (12)	Eu1—I2	3.281 (17)
Eu1—I1^{i}	3.472 (6)	Eu1—I2^{iii}	3.365 (17)
Eu1—I1^{ii}	3.311 (12)		

Symmetry codes: (i) $-x+1, y+\frac{1}{2}, -z+1$; (ii) $-x+\frac{1}{2}, -y+1, z+\frac{1}{2}$; (iii) $-x+\frac{1}{2}, -y+1, z-\frac{1}{2}$.

Total-energy density-functional calculations were performed using plane waves/pseudopotentials and the computer program *VASP* (Vienna *ab initio* package; Kresse & Furthmüller, 1996*a*,*b*; Kresse & Hafner, 1993) employing the generalized gradient approximation (GGA) of PBE type (Perdew *et al.*, 1996) and the projected–augmented wave (PAW) method (Blöchl, 1994). The cut-off energy was set at 500 eV. All four cells were allowed to change in volume and shape, and all atomic positions were allowed to relax. The convergence criterion of the electronic-structure calculation was chosen as 10^{-5} eV because of the expected small energy differences in the calculated structures.

Data collection: *WinXPow* (Stoe & Cie, 2005); cell refinement: *WinXPow*; data reduction: *WinXPow*; program(s) used to solve structure: *FULLPROF* (Rodriguez-Carvajal, 1993); program(s) used to refine structure: *FULLPROF*; molecular graphics: *ATOMS* (Dowty, 2005); software used to prepare material for publication: *enCIFer* (Allen *et al.*, 2004).

Financial support by the Deutsche Forschungsgemeinschaft (DFG) is gratefully acknowledged.

Supplementary data for this paper are available from the IUCr electronic archives (Reference: SQ3214). Services for accessing these data are described at the back of the journal.

References

Allen, F. H., Johnson, O., Shields, G. P., Smith, B. R. & Towler, M. (2004). *J. Appl. Cryst.* **37**, 335–338.
Bärnighausen, H. & Schulz, N. (1969). *Acta Cryst.* B**25**, 1104–1110.
Beck, H. P. (1979). *Z. Anorg. Allg. Chem.* **459**, 81–86.
Blöchl, P. E. (1994). *Phys. Rev. B*, **50**, 17953–17979.
Dowty, E. (2005). *ATOMS*. Version 6.2. Shape Software, Kingsport, Tennessee, USA.
Howell, J. K. & Pytlewski, L. L. (1969). *J. Less Common Met.* **18**, 437–439.
Kresse, G. & Furthmüller, J. (1996*a*). *Comput. Mater. Sci.* **6**, 15–50.
Kresse, G. & Furthmüller, J. (1996*b*). *Phys. Rev. B*, **55**, 11169–11186.
Kresse, G. & Hafner, J. (1993). *Phys. Rev. B*, **47**, 558–561.
Liu, G. & Eick, H. A. (1989). *J. Less Common Met.* **156**, 237–245.
Perdew, J. P., Burke, K. & Ernzerhof, M. (1996). *Phys. Rev. Lett.* **77**, 3865–3868.
Rodriguez-Carvajal, J. (1993). *Physica B*, **192**, 55–69.
Stoe & Cie (2005). *WinXPOW*. Version 2.23. Stoe & Cie, Darmstadt, Germany.
Wang, L., Wang, S., Zhao, X. & Sun, J. (1995). *J. Alloys Compd*, **225**, 174–177.